Modeling Study of Herringbone Gear Gap Space Borrow and Grinding Wheel Max Diameter Determination

Zemin Zhao (zeminzhao666@163.com)
AECC Harbin Dongan Engine CO., LTD. https://orcid.org/0000-0003-2326-0596
Xingfu Zhao
AECC Harbin Dongan Engine CO.,LTD.
Hao Sun
AECC Harbin Dongan Engine CO.,LTD.
Chao Dong
AECC Harbin Dongan Engine CO.,LTD.
Chunlei Wang
AECC Harbin Dongan Engine CO., LTD.
Shancheng Wang
Aero Engine Corporation of China Harbin Dongan Engine CO.,LTD.
Hongyan Zhang
AECC Harbin Dongan Engine CO., LTD.

Research Article

Keywords: herringbone gear grinding, gear gap borrow grinding, undercut width design, grinding wheel maximum diameter

Posted Date: March 14th, 2022

DOI: https://doi.org/10.21203/rs.3.rs-1329305/v1

Modeling study of herringbone gear gap space borrow and grinding wheel max diameter determination

Title page

Order	Author Name	Email	Title
1	Zemin Zhao	zeminzhao666@163.com	Dr & Engineer
2	Xingfu Zhao	13796014387@139.com	Senior Engineer
3	Hao Sun	18145144698@163.com	Senior Engineer
4	Chunlei Wang	wangchunlei2006@126.com	Senior Engineer
5	Chao Dong	18745788579@126.com	Senior Engineer
6	Shancheng Wang	dadlwsc@163.com	Senior Engineer
7	Hongyan Zhang	hongyanzhang666@163.com	Engineer

Institution：AECC HARBIN DONGAN ENGINE CO. , LTD.

Corresponding Author：Zemin Zhao

Abstract

In aviation, the machine quality and accuracy of herringbone gear are strictly required, and its realization depends on the grinding process. There is an urgent need for further expansion of grinding wheel diameter. This paper proposed a gear gap space borrow grinding method and determined the analyzing relation between grinding wheel diameter and herringbone gear design parameters. Based on certain assumptions and idealized processing methods, the method of the gear undercut width design and the wheel maximum diameter determination are completed by geometry modeling combining the analytical and simulation method. After solid contact simulation verification, several important phenomena have been discussed, then valuable laws and conclusions have been obtained.
Keywords: herringbone gear grinding; gear gap borrow grinding; undercut width design; grinding wheel maximum diameter;

0. Instruction

Herringbone gear takes into account the characteristics of smooth transmission of helical gear, at the same time, it has strong bearing capacity, and also has the characteristics of overcoming the axial force generated by helical gear. At present, Herringbone gear has strong special demand in the field of aviation[1].

As an important part in aviation field, the machining process of herringbone gear is often accompanied by grinding due to its high material strength and high processing quality requirements. The diameter of grinding wheel is the main factor for grinding quality and efficiency, generally, larger wheel diameter means higher grinding quality and efficiency. for higher specific power, Aviation transmission parts tends to miniaturization and lightweight. The shrink of volume and space limits the further extension of the wheel diameter. The contradiction between smaller gear and lager wheel diameter under high processing quality and high specific power are becoming more prominent.

The advantages of expanding grinding wheel diameter are significant. The increase of wheel diameter means a certain improvement of grinding quality, wheel strength, wheel dressing allowance and service life. The study of grinding wheel diameter further extension in limited condition is necessary.

In this paper, the concept and method of gear gap space borrow grinding are proposed for the first time. The quantification and implementation method of gear gap borrow grinding are the contact problem of multiple entity characteristics.

Contact simulation based on solid modeling is the most direct method, but custom model building for different herringbone gears are poor timelines, or secondary development based on solid building software needs long term of development cycle and extreme cost. Otherwise, the debugging process during simulation may accompany with some human observation.

In recent years, the solid simulation method is mostly used in the force analysis of gears, not in the contact analysis. Sagar Patil and Prashant Ambhore[1] display 3D herringbone gears by utilizing CATIA V5 software programming, and the different typical materials are defined in ANSYS software, then the stress analysis and twisting of the gears are checked and analyzed. Ke Li[3] undertakes the modeling and assembling of a herringbone gear by using UG software. Meshing characteristics of the gears assembly model under static state were concluded through the ANSYS software. Simulation analysis on the herringbone gear meshing force was conducted to verify the gear design rationality.

Analytical modeling method based on curve equations can describe the geometry relation quantitatively, but the profile mathematical model of the gear tooth and grinding wheel need to be

constructed by multiple piecewise functions, which results in a complex model after a couple of substitutions. Before solving the intersection point, the parameter interval of possible intersecting piecewise function needs to be distinguished based on the complex models consist of piecewise functions by which is too inconvenient for solving the contact problem with uncertain intersection point.

Feng, G. et al. [4] developed a three-dimensional mathematical model to analyze the characteristics of herringbone face-gear drives, including the tooth contact area, the axial force on the pinion gear, the contact ratio. et al. Shangjun Ma et. al. [5] combines the accurate parameterized modeling and Pro/E software to establish a herringbone gear with high accurate involutes and tooth root transition circular curve. Finite element calculation and dynamic analysis proves the gear model is accurate enough for kinematics and dynamics analysis.

This paper tends to combine the advantages of above two methods, in order to avoid the tedious simulation process and piecewise function application, the model building process only bases on the geometry spatial position relations between gear and wheel, and the solid contact simulation is also applied only for reference, validation and improving the visibility of quantity debug process.

1. Herringbone gear gap space borrow grinding method

1.1 The quantitative description of gear gap space borrow grinding

As shown in Fig. 1 (a), the herringbone gear is composed of two group of helical gear with opposite rotation. In order to meet the requirements of machining process, an undercut is generally constructed between the gears, which also provides a certain space for the diameter extension of grinding wheel at the same time. At present, the wheel diameter extension method based on wider undercut width is the most commonly used, which results in a proportional increase in mass and axial size of the aviation parts.

As shown in Fig. 1 (b) and (c), the typical grinding machining mode of herringbone gear has been basically cured, there is no other possibility to expand wheel diameter on grinding machine structure and motion pair.

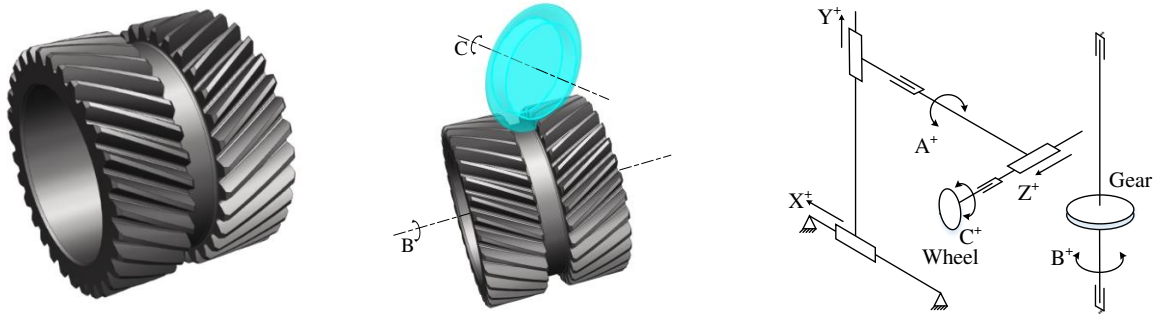

(a)Typical herringbone gear (b)Position relation in grinding (c)Equipment structure and motion pair

Fig. 1 Structure and grinding process of herringbone gear

As shown in Fig. 2, after a period of simulation research, another wheel diameter extension possibility comes from herringbone gear itself has been found. Under certain appropriate design parameters of undercut width and helical angle, it is still possible to borrow the opposite gear gap space or opposite and adjacent gear gap space to further improve the diameter of grinding wheel, as shown in Fig. 2 (a) and (c).

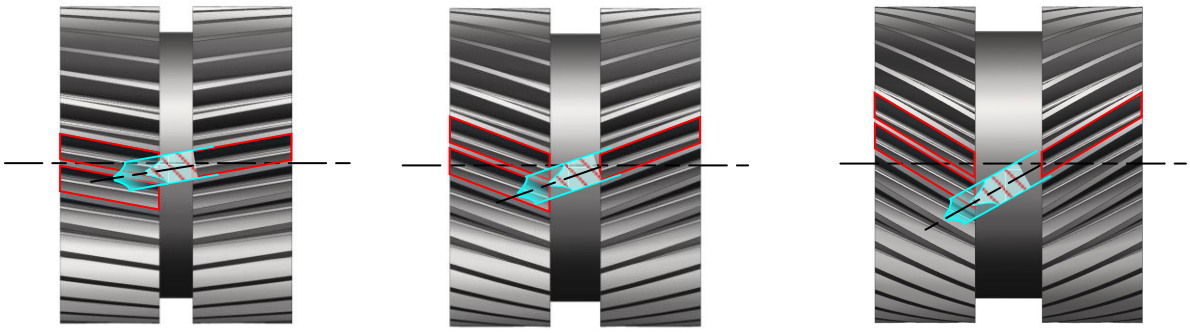

(a) borrowing opposite gap space (b) borrowing undercut space (c) borrowing opposite and adjacent gap

Fig. 2 borrow gap forms of grinding wheel

Therefore, this study intends to further expand the grinding wheel diameter by gap space borrowing, and the possibility above need to be described quantitatively. The contact simulation based on secondary development method has a directly visible debug process, but expensive and time consuming, and the pure analytical method is too complex to solve. After a period of research, modeling method based on geometry relations were applied to describe the relation of key parameters, as shown in Fig. 3. The possibility of gap space borrow grinding depends on the interface position of grinding wheel and gear gap.

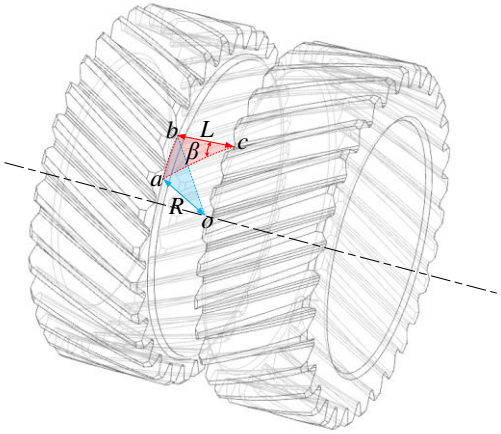

Fig. 3 Key parameters of herringbone gear on cylinder of pitch circle

As shown in Fig. 3, the values marked in curved triangle $\triangle abc$ are coplanar with cylinder of pitch circle, L is undercut width, β is helical angle. In end face sector *abo*, R is radius of gear pitch circle. If assume that the grinding wheel can borrow the opposite adjacent gap space in this situation, the wheel comes from point *c* opposite the point *b* must be able to intervene in the gap space at point *a*. It means the length of *arc ab* is an integer multiple of the gear pitch. Due to the thickness of grinding wheel is less than width of gap space in general, the multiples have allowance that float around integers. Given that the value rang and float range of the multiples must be discussed and determined, assuming the multiples as the parameter K. According to the geometry relation above, the pitch can be expressed by normal module m_n, number of teeth z, radius of pitch circle R, the *arc ab* can be expressed by L and β. The multiple relation of pitch and *arc ab* is described by K, after substitution and simplification, the relation of key parameters is shown as formula (1).

$$L = K \cdot \frac{\pi \cdot m_n}{\sin \beta} \tag{1}$$

Gap borrow grinding condition has been quantified as index K, as shown in Fig. 4, different integer K represents different gap space borrowing. But due to the geometry contact characters, the intersection of the grinding wheel and gear profile is possible only to a limited extent. As shown in Fig. 4, the wheel gradually deviate from the gear with the increase of K. parameter K can be regarded as the indicator to judge the possibility of gap space borrow and interference. In order to determine value range of K initially, the departure function H (K) should be established.

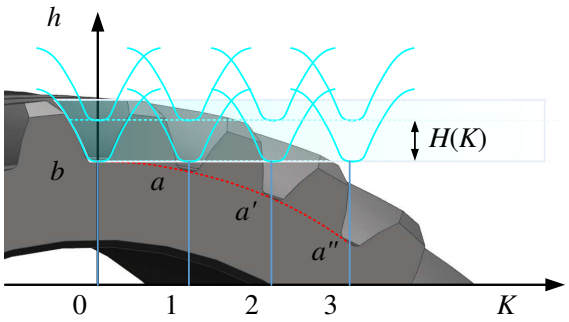

Fig. 4 Interface and gap borrow relation of herringbone gear grinding

According to the profile geometry relation of grinding wheel and herringbone gear, the departure function can be built initially as formula (2).

$$H = \frac{\sqrt{L \cdot (m_n \cdot z - L)}}{\cos \beta} \tag{2}$$

After substituting formula (1) into formula (2), H (K) has been deduced as formula (3).

$$H = \frac{m_n \cdot \sqrt{K \cdot \pi \cdot (z \cdot \sin \beta - K \cdot \pi)}}{\sin \beta \cdot \cos \beta} \tag{3}$$

Essentially, the deduced values L, H and K are both functions of the key parameters z, m_n, β and R. The gap space borrow condition has been abstracted as parameter K and its boundary constrained function H. In order to determine implication of K value, numerical simulation of key parameters in common value range must be implemented and explored.

1.2 The numerical implication study of gap space borrow indicator

From the above modeling perspective, parameter K is the indicator that measures the possibility of gap space borrowing. Fig. 5 is the numerical distribution of parameter K in transverse projection, which is built based on Fig. 4 by projection and transmission.

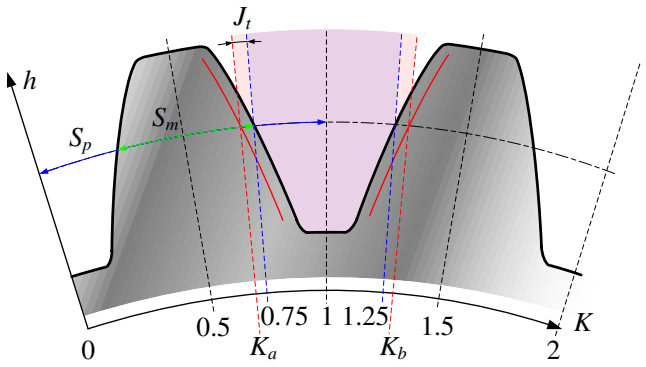

Fig. 5 Numerical distribution of parameter K in transverse projection

Based on MATLAB software, after vast numerical and geometry simulations have been implemented on formula (1) and (3), an important rule of K has been discovered that the available gap space borrow interval is always between K_a and K_b, which are the interaction points of gear involute profile and pitch circle, as shown in Fig. 5. The rule of K above results in the influence of the grinding wheel thickness and gear profile relative torsion, which will be studied closely in section 3.

As shown in Fig. 5, the position of integers and half integers as set {0, 0.5, 1, 1.5, 2} of parameter K is constant in any herringbone gear based on formula (1). In the fixed gear center distance assembly, gear dressing operation is carried out to ensure the tooth side gaps[6][7]. Under the influence of tooth side gaps J_t, the values of K_a and K_b depend on the arc length of pitch S_p and tooth thickness S_m. Besides, given that the difference of actual parts and ideal model, the safety margin δ should be considered. After the J_t of tooth thickness S_m is removed, the K_a and K_b can be expressed as set (4).

$$\begin{cases} K_a = 0.75 - \dfrac{J_t}{S_p} + \delta \\ K_b = 1.25 + \dfrac{J_t}{S_p} - \delta \end{cases} \tag{4}$$

For declare the specific implication of parameter K, K needs to be assigned a specific value. The S_p is equal to $2 \cdot S_m$ of standard gear in design stage before dressing, in which the specific values of K_a and K_b can be determined to be 0.75 and 1.25. When the gear is in the design stage before dressing. Based the vast numerical simulations and tests above, the range deserve discussion of K is determined in [0, 1.75), the K over 1.75 presents the wheel and gear will separate from each other due to the circular shape. The gap borrow condition is most sensitive to the change of helical angle, the range of helical angle is the main factor for the determination of the optimal K value. The numerical distribution table of K as shown in Table. 1.

Table. 1 Numerical distribution table of K

K	Gap borrow mode	Implementation assessment
[0,0.25)	Opposite gap space	Infrequent，β is below usual range
[0.25,0.75)	Interferes opposite gear profile	Unavailable
[0.75,1.25)	Opposite and adjacent gap space	Common, $\beta \in (15°, 35°)$
[1.25,1.75)	Interferes opposite and adjacent profile	Unavailable
[1.75, +∞)	No interface & No gap borrow	Infrequent，β is out of usual range

In in Table. 1, the meaning of K values is revealed. In common range of key parameters, K in [0.25,0.75) and [1.25,1.75) is unavailable for gap borrow grinding. When K is in [1.75, +∞), the grinding wheel is completely separated from the profile of the gear. In [0,0.25), the value of β is too small to exploit the mechanical advantages of the helical gear, and K=0 means β=0, neither of them is worth studying. In conclusion, the interval [0.75,1.25) of K is the most significant range of discussion and application, at the same time, $\beta \in (15°, 35°)$ is also commonly used in aviation helical gears. besides, the integer of K in [0.75,1.25) is K=1, which is the optimal gap borrow situation in theory, but not in actual process due to the effects of tooth distortion and grinding wheel boundary tilt in subsequent study.

The gap borrow grinding conditions are abstracted to the numerical value of K, the final value K is the calculation result of different key parameters combination. The gap borrow grinding conditions can be determined by the K of key parameters combination, in return, the key parameters combination can also be optimized by the control of K to achieve a design of available gap borrow herringbone gear. When K=1, the map surface and partitions of key parameters is established as shown in Fig. 6.

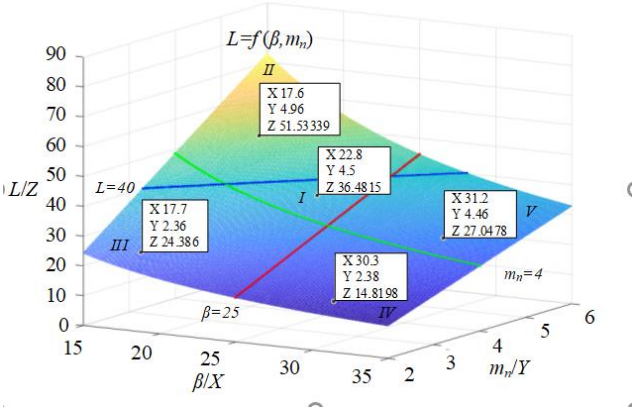

Fig. 6 Map surface and partitions of L、β and m_n

All the key parameter combinations on the map surface are at the optimal gap borrow grinding situation in theory, the herringbone gears of available gap borrow grinding can be initially designed based on the parameter partitions. The Fig. 6 based on formula (1) and Table. 1 improves the visibility of parameter design process to a certain extent.

Based on the above quantity relation，the gap borrow conditions of existing herringbone gears can be determined, and more meaningfully, the method can also coordinate the design process to achieve the herringbone gear design of available gap borrow grinding.

2. The maximum diameter modeling of gap borrowing grinding wheel

Before the herringbone gear grinding process, repeated grinding test and wheel dressing for a proper wheel size consume plenty of time, and wheel size determination mainly depends on human observation. Neither accuracy and efficiency can be guaranteed. Grinding wheel size, especially the diameter is the key parameter for grinding efficiency and quality, however, there is no accurate diameter determination method for gap borrow grinding even for undercut borrow grinding.

As shown in Fig. 7, the solution of wheel diameter D needs to be implemented on $\triangle abo$, the modeling of intermediate function relies on the contact relation of wheel and gear.

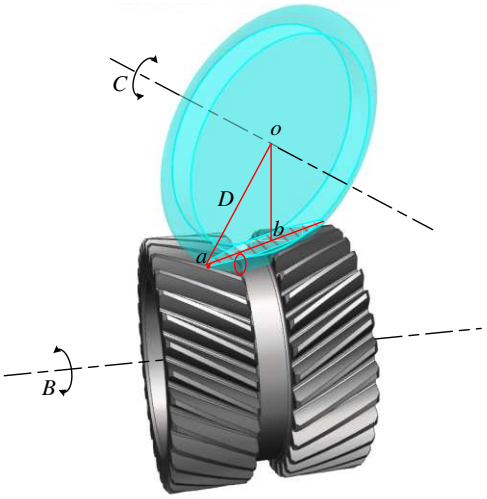

Fig. 7 The contact and geometry relation of grinding wheel and herringbone gear.

In fact, the gap space borrow is a further space borrow operation on the basis of traditional undercut space borrow, the wheel diameter determining model of undercut space borrow grinding should be built firstly.

2. 1 Modeling of grinding wheel maximum diameter of undercut borrow grinding

As shown in Fig. 8 is the geometry contact relation of herringbone gear and grinding wheel radius in undercut borrow grinding, the grinding wheel diameter can be determined in $\triangle dco'$.

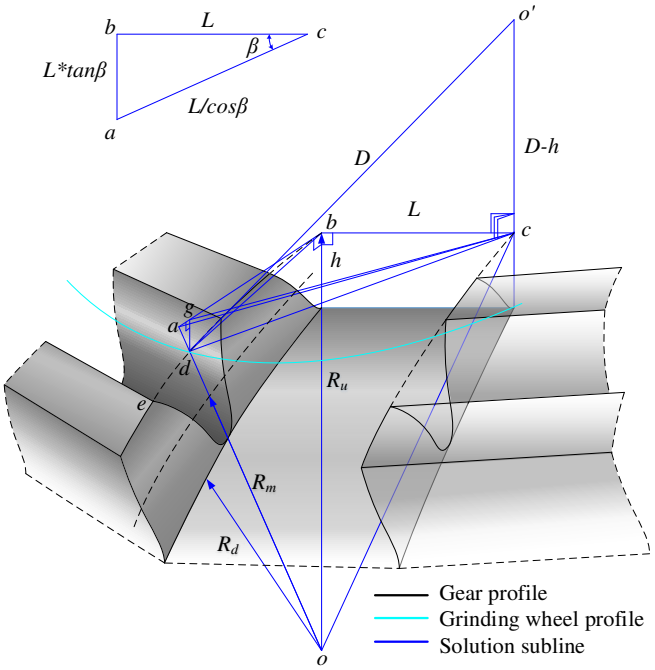

Fig. 8 The geometry contact relation of herringbone gear and grinding wheel radius in undercut borrow grinding

Based on the triangle relation in $\triangle abc$, $\triangle abo$, $\triangle obc$, the following sets of equations are deduced, as shown in formula (5). Where, the R_u is the radius of addendum circle.

$$\begin{cases} ab = L \cdot \tan\beta \\ ac = L/\cos\beta \\ ao = \sqrt{R_u{}^2 + ab^2} \\ co = \sqrt{R_u{}^2 + L^2} \end{cases} \tag{5}$$

Then, the intersect angle of edge *ac* and edge *ao* is built by applying cosine law in △*aoc*, shown as formula (6).

$$\cos\angle cao = \frac{ac^2 + ao^2 - co^2}{2 \cdot ac \cdot ao} \tag{6}$$

Similarly, the chord length of wheel radius is 2·*cd*, where, is shown as formula (7).

$$cd = \sqrt{ac^2 + ad^2 - 2 \cdot \cos\angle cao \cdot ac \cdot ad} \tag{7}$$

And $ad=ao-R_u$, in order to solve diameter *D* in △*dco′*, the angle ∠*dco′* must be determined firstly. Line *dg* and line *co′* are collinear, the angle ∠*dco′* can be derived into formula (8).

$$\angle dco' = \frac{\pi}{2} + \angle gcd \tag{8}$$

Where the angle ∠*gcd* in formula (8) can be expressed as formula (9) in △*adg*.

$$\angle gcd = a\sin(\frac{gd}{cd}) \tag{9}$$

And where the lines *gd* in formula (9) is shown in formula (10) based on geometry relation.

$$\begin{cases} gd = ad \cdot \cos\angle gda \\ \angle gda = 2 \cdot \pi / Z \end{cases} \tag{10}$$

Applying cosine law in △*dco′*, the grinding wheel diameter *D* of undercut space borrow grinding is finally solved as formula (11) shown.

$$D = \frac{2 \cdot \cos(\angle dco') \cdot cd \cdot h + cd^2 + h^2}{cd \cdot \cos(\angle dco') + h} \tag{11}$$

2.2 Modeling of grinding wheel maximum diameter of gap space borrow grinding

Based on the wheel diameter model and modeling method of undercut borrow grinding, the grinding wheel diameter D_{Max} of opposite and adjacent gap space borrow can be determined in triangle △*fco′*, as shown in Fig. 9. But the difference is that line *cd* and line *cf* intersect at points *c*, but do not coincide. Although the angle of line *cd* and line *cf* is small, its value may fluctuate seriously with the change of gear parameters. This error cannot be ignored for the accurate solution of diameter D_{Max}.

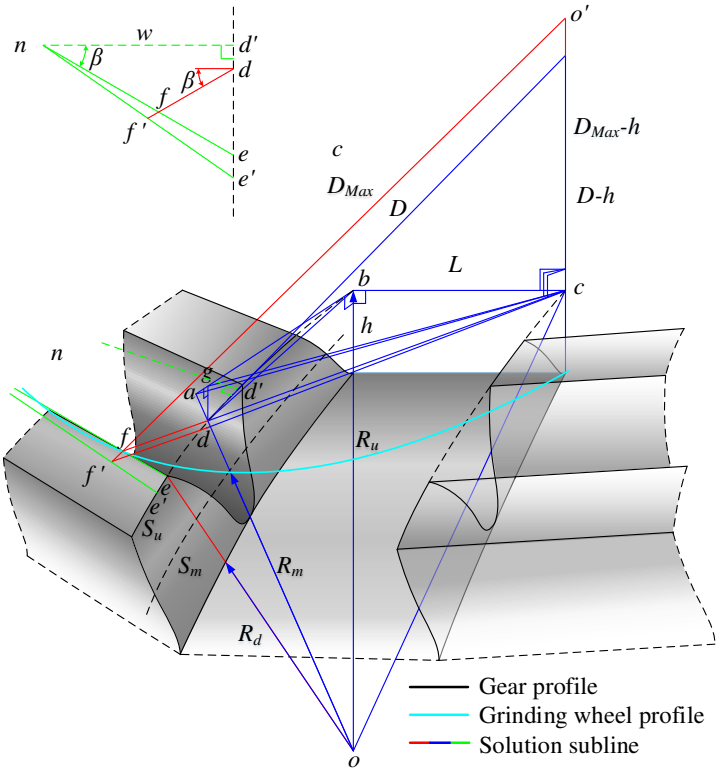

Fig. 9 The geometry contact relation of herringbone gear and grinding wheel radius in gap space borrow grinding

In addition, the distortion of helical gear on the base circle cylinder must be considered. As shown in Fig. 9, the extension cord of line *cd* does not intersect with the line *ef*. The plane on which the triangle $\triangle fco'$ is actually intersect at point f' with the gear top line $f'e'$ after distortion.

In the expanded curved triangle $\triangle d'ne'$, the length of ee' is a part of arc $e'd'$. based the triangle relation and arc length formula, the following sets of equations are built as formula (12), where w is the width of gear.

$$\begin{cases} ee' = w \cdot \tan\beta \cdot (\dfrac{R_u}{R_m} - 1) \\ en = w/\cos\beta \\ e'n = \sqrt{en^2 + ee'^2 + 2 \cdot en \cdot ee' \cdot \sin\beta} \end{cases} \tag{12}$$

In triangle $\triangle f'de'$, the absolute depth of wheel borrowing gap space df' is deduced as formula (13) according to the sine law.

$$df' = \frac{\sin(\angle ne'e) \cdot e'd}{\cos(\beta - \angle ne'e)} \tag{13}$$

Where, the function expression of the intermediate substitution is as formula (14).

$$\begin{cases} \angle ne'e = arc\sin(\dfrac{w}{e'n}) \\ e'd = ee' + ed \end{cases} \tag{14}$$

The distortion of gear top line *fe* also results in a descending of point *f* to point *f ′* along the radius direction. The descending distance f_D is deduced as formula (15).

$$f_D = \sqrt{(df \cdot \sin\beta)^2 + R_u^2} - R_u \tag{15}$$

Then, the angle of line *cd* and *cf* line can be expressed as formula (16).

$$\angle fcf' = \arctan(\frac{f_D}{df + cd}) \tag{16}$$

In order to determine the D_{Max} in triangle $\triangle fco'$, the line *df* of formula (15) and formula (16) must be quantified firstly in the curved triangle $\triangle def$. Otherwise, the line *ed* of formula (14) can also be quantified in equation sets (17).

$$\begin{cases} ed = \dfrac{\pi \cdot R_u}{Z} - \dfrac{S_u}{2} \\ df = \dfrac{ed}{2 \cdot \sin\beta} \end{cases} \tag{17}$$

Where, R_u is radius of gear top circle. According to the calculation formula of gear, the circular tooth thickness of gear top circle S_u can be expressed as formula (18).

$$S_u = R_u \cdot (\frac{S_m}{R_m} + 2 \cdot inv\alpha - 2 \cdot inv\alpha_u) \tag{18}$$

The S_m and R_m is the circular tooth thickness and radius of the pitch circle respectively. The expression of them are shown as equation sets (19).

$$\begin{cases} S_m = \dfrac{\pi \cdot m_n}{2 \cdot \cos\beta} \\ R_m = \dfrac{m_n \cdot Z}{2 \cdot \cos\beta} \end{cases} \tag{19}$$

And the substitution $inv\alpha$ and $inv\alpha_u$ in equation sets (19) is shown in sets (20).

$$\begin{cases} inv\alpha = \tan\alpha - \alpha \\ inv\alpha_u = \tan(a\cos(\dfrac{R_m}{R_u} \cdot \cos\alpha)) - a\cos(\dfrac{R_m}{R_u} \cdot \cos\alpha) \end{cases} \tag{20}$$

Finally, in triangle $\triangle fco'$, the grinding wheel diameter of opposite and adjacent gap borrow is expressed as formula (21).

$$D_{Max} = \frac{2 \cdot \cos(\angle f'co') \cdot f'c \cdot h + f'c^2 + h^2}{f'c \cdot \cos(\angle f'co') + h} \tag{21}$$

Where the substitution as shown in sets (22).

$$\begin{cases} \angle f'co' = \angle fcf' + \angle fco' \\ f'c = \dfrac{df' + cd}{\cos(\angle fcf')} \end{cases} \tag{22}$$

The modeling process of D_{Max} includes assumptions and omissions, model defects and errors need to be compensated and modified combining with machining process.

3. Modification and compensation of gap space borrow grinding

3.1 Modification grinding wheel thickness and side contact

As shown in Fig. 10 (a), the value of K usually fluctuates around value 1 due to the round-off number of design parameters and the real thickness of grinding wheel, which less than the gap width as shown in Fig. 10 (b). Simulation proves that the parameters fluctuation, side space of wheel and profile rotation of opposite and adjacent gap results in complex contact and interference, which is difficult to be expressed clearly by analytical method. After series of contact simulation, the contact or interference between grinding wheel profile and gear profile or tooth surface eventually manifests as sine like curve $e'd'$ formed by the projection vertex of grinding wheel, which also stands for the difference of gap borrowing effect, as shown in Fig. 10 (a).

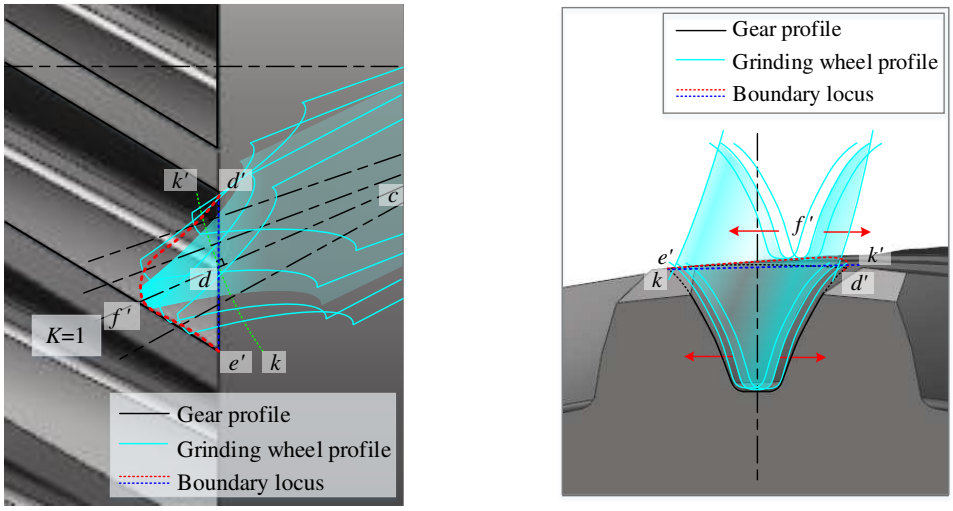

(a) Wheel top boundary of gap borrow in different K

(b) The side moving and contact of grinding wheel

Fig. 10 Gap space borrow efficiency in practice

The length of line $f'c$ is consist of line $f'd$ and line cd, both of them change with the helical angle β. The curve consists of point e', d and d' approximates the line $e'd'$, the variation of line cd on line $e'd'$ can be assumed as linear function as shown in Fig. 10 (a). To avoid the analytical calculation of the complex contact or interference, this paper constructs the approximate change coefficient function of line $f'd$ and line cd according the simulation results. After projection, the functions of the curve $e'd'$ and line

$e'd'$ are constructed as equation sets (23).

$$\begin{cases} U = \left|\cos(2 \cdot K \cdot \pi)\right| \\ V = \dfrac{(K-1) \cdot \sin^2 \beta}{L} + 1 \end{cases} \tag{23}$$

As shown in Fig. 11, the function types are consistent and the functions accuracy are also sufficient.

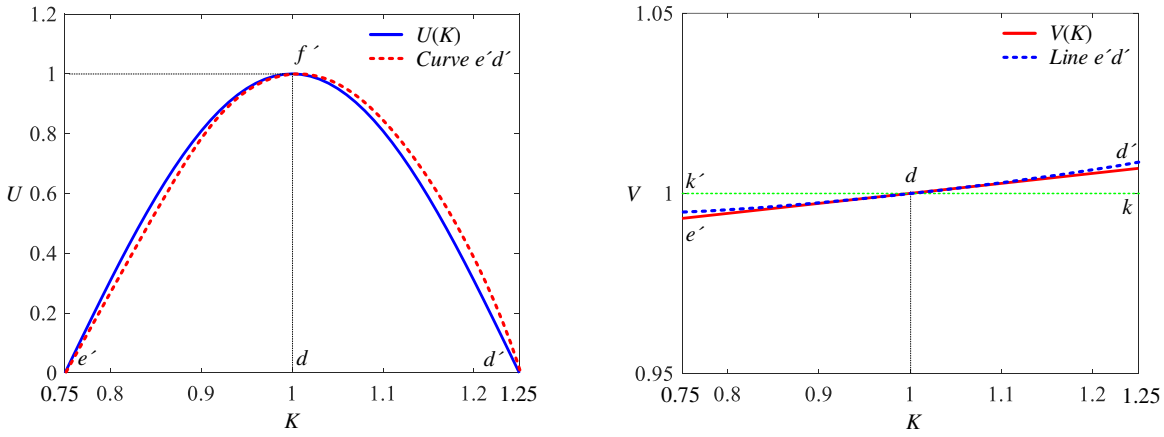

(a) Coefficient function $U(K)$ (b) Coefficient function $V(K)$

Fig. 11 Construction and verification of coefficient functions

In addition, the modified line $f'c$ can be expressed as formula (24).

$$FC = \frac{U \cdot df' + V \cdot cd}{\cos(\angle f'cf)} \tag{24}$$

The formula (21) can be updated as formula (25).

$$D_{Max} = \frac{2 \cdot \cos(\angle f'co') \cdot FC \cdot h + FC^2 + h^2}{FC \cdot \cos(\angle f'co') + h} \tag{25}$$

3.2 Compensation of grinding wheel lifting space

This study means to determine the maximum diameter of grinding wheel, but in machining process, the lifting space of the wheel must be considered. As shown in Fig. 12, the minimum lifting space consists of I_C for the wheel lifting and E_D for ensuring all gear surface grinding, which needs the axis C translate from point c to point c' firstly.

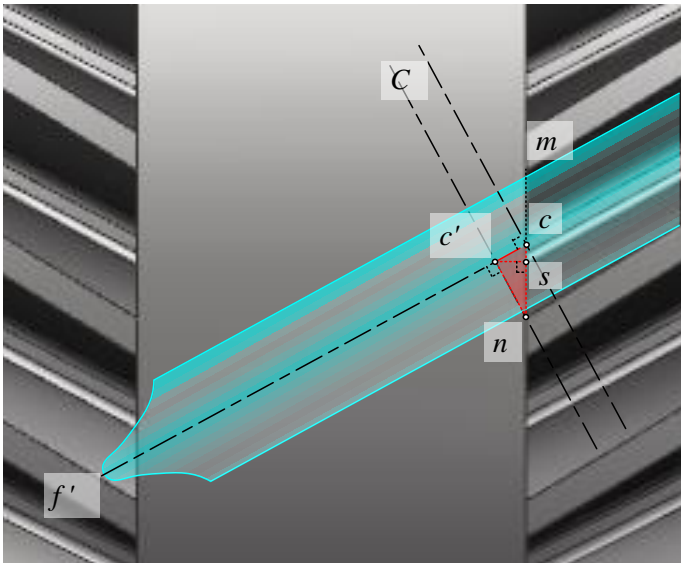

Fig. 12 Compensation of grinding wheel lifting space

Assuming the length of line $c'c$ and line $c's$ as E_D and the E_L, the expression of them is shown as equation sets (26).

$$\begin{cases} E_D = C_{cn} \cdot \sin\beta \\ E_L = C_{cn} \cdot \sin\beta \cdot \cos\beta \end{cases} \tag{26}$$

Where, C_{cn} is the half chord length of gap space as shown in formula (27).

$$C_{cn} = R_u \cdot \sin\left(\frac{\pi}{z} - \frac{S_u}{2 \cdot R_u}\right) \tag{27}$$

Besides the E_D there is another necessary space in lifting space I_C comes from arc grinding out path for avoiding the inertia collision, which usually determined in CNC programming process. When the compensation is applied in the determination of the wheel maximum diameter D and D_{Max}, they can be updated as equation sets (28).

$$\begin{cases} D = \dfrac{2 \cdot \cos(\angle dco') \cdot (cd - E_D - I_C) \cdot h + (cd - E_D - I_C)^2 + h^2}{(cd - E_D - I_C) \cdot \cos(\angle dco') + h} \\ D_{Max} = \dfrac{2 \cdot \cos(\angle f'co') \cdot (FC - E_D - I_C) \cdot h + (FC - E_D - I_C)^2 + h^2}{(FC - E_D - I_C) \cdot \cos(\angle f'co') + h} \end{cases} \tag{28}$$

CNC programming research is not covered in this paper, the value of I_C in later verification and discussion is ignored.

3.3 Verification based on simulation

There are a variety of cases of interference between herringbone gear and grinding wheel, as shown in Fig. 13. The study in this paper approximates the interference relations above by fitting function, which requires accuracy verification.

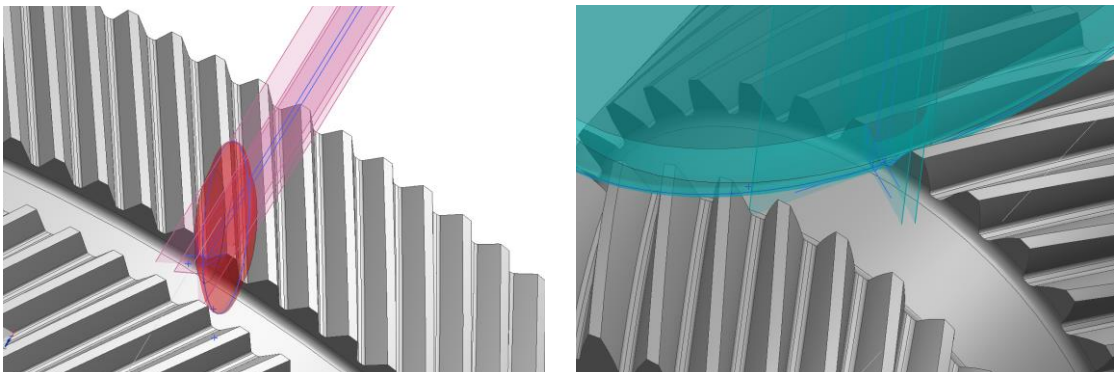

(a) Interference of grinding wheel thickness (b) Interference of grinding wheel flange

Fig. 13 Solid simulation process for model verification

Solid contact simulation based on UG software has been performed on twelve typical herringbone gear. Different parameters of the gear and lifting space distances of the wheel are shown in Table. 2, where the value of E_D and E_D' comes from model calculation and contact simulation respectively.

Table. 2 Herringbone gear parameters and lifting space distance evaluation

Herringbone	m_n	β(°)	α(°)	Z	w(mm)	L(mm)	Φ_u(mm)	Φ_d(mm)	E_D(mm)	E_D'(mm)	Error(%)
Gear 1	3.8788	30	22.5	27	47	20	130.595	108.5	3.183	3.281	2.987
Gear 2	3.8788	30	22.5	118	47	20	537.42	515.317	2.771	3.0	7.633
Gear 3	2.514	30	22.5	27	30	20	85.305	71.15	2.181	2.168	0.600
Gear 4	2.514	30	22.5	106	30	20	312.68	298.55	1.711	1.911	10.466
Gear 5	2.75	30	22.5	33	38	20	110.265	97.81	1.987	2.073	4.149
Gear 6	2.75	30	22.5	115	38	20	370.62	358.2	1.862	1.954	4.708
Gear 7	4.25	30	22.5	31	61	20	160.605	141.41	3.088	3.221	4.129
Gear 8	4.25	30	22.5	130	61	20	646.42	627.25	2.872	3.012	4.648
Gear 9	4	30	22.5	34	48	20	165.8	147.8	3.005	3.04	1.151
Gear 10	4	30	22.5	31	48	20	151.183	133.183	2.911	3.031	3.959
Gear 11	1.56	30	22.5	36	16.6	15	68.075	60.98	1.137	1.174	3.152
Gear 12	1.56	30	22.5	48	16.6	15	89.425	82.33	1.077	1.143	5.774

As shown in Table. 2, the errors between E_D and E_D' are small enough, and the average relative error is 4.45%, which is consistent with the modeling requirements. E_D as an intermediate variable, its accuracy has been verified, which indicates that the accuracy of the whole model has also been partially proved.

The gear gap space borrowing condition K, K_a and K_b, space borrow efficiency V, the diameter of the wheel with the E_D and interference in consideration are shown in Table. 3. D and D' are the wheel diameter without gear gap borrow, which come from model calculation and contact simulation respectively. D_{Max} and D_{Max}' are the wheel diameter with gear gap borrow, which come from model calculation and contact simulation respectively.

Table. 3 Herringbone gear gap borrow condition and diameter evaluation

Herringbone	K	(Ka, Kb)	Gap space borrow	V	D(mm)	D'(mm)	Error(%)	D_{Max}(mm)	D_{Max}'(mm)	Error(%)
Gear 1	0.821	(0.746, 1.254)	Available	0.998	48.745	49.195	0.915	64.334	68	5.391
Gear 2	0.821	(0.746, 1.254)	Available	0.998	48.938	48.186	1.573	59.037	63	6.29
Gear 3	1.266	(0.745, 1.256)	Unavailable	1.003	80.705	86.609	6.817	——	——	——
Gear 4	1.266	(0.745, 1.255)	Unavailable	1.003	75.974	75.051	0.132	——	——	——

Gear 5	1.158	(0.746, 1.255)	Available	1.002	90.617	93.961	3.559	118.422	128.159	7.598
Gear 6	1.158	(0.745, 1.255)	Available	1.002	82.469	82.514	0.055	100.243	102.66	2.354
Gear 7	0.749	(0.747, 1.253)	Available	0.997	53.629	53.979	0.648	53.691	52	3.252
Gear 8	0.749	(0.747, 1.253)	Available	0.997	52.872	52.462	0.782	52.764	55	4.065
Gear 9	0.796	(0.747, 1.253)	Available	0.997	56.588	57.341	1.313	67.52	67	0.776
Gear 10	0.796	(0.747, 1.253)	Available	0.997	57.32	57.728	0.707	68.15	68	0.221
Gear 11	1.53	(0.741, 1.259)	Unavailable	1.009	103.596	111.467	7.061	——	——	——
Gear 12	1.53	(0.741, 1.259)	Unavailable	1.009	96.946	100.921	3.939	——	——	——

As shown in Table. 3, the relative errors of D and D_{Max} are both under 10% with the average error 3.43% and 3.74% respectively, which is accurate enough for theoretical modeling study. The correctness and accuracy of equation sets (28) include formula (11) and formula (25) are verified. The approximation and hypothesis operation during modeling process of them are also proved to be reasonable and proper.

3.4 Discussion based on verification

Through the process of verification based solid contact simulation, several phenomena worth discussing can be observed. The herringbone gears available for gap borrow and their borrow efficiency are shown in Table. 4.

Table. 4 Efficiency evaluation of gear gap borrow

Herringbone	K	(K_a, K_b)	V	D(mm)	D_{Max}(mm)	Improvement (%)
Gear 1	0.821	(0.746, 1.254)	0.998	48.745	64.334	31.981
Gear 2	0.821	(0.746, 1.254)	0.998	48.938	59.037	20.636
Gear 5	1.158	(0.746, 1.255)	1.002	90.617	118.422	30.684
Gear 6	1.158	(0.745, 1.255)	1.002	82.469	100.243	21.552
Gear 7	0.749	(0.747, 1.253)	0.997	53.629	53.691	0.116
Gear 8	0.749	(0.747, 1.253)	0.997	52.872	52.764	-0.204
Gear 9	0.796	(0.747, 1.253)	0.997	56.588	67.52	19.319
Gear 10	0.796	(0.747, 1.253)	0.997	57.32	68.15	18.894

As shown in Table. 4, not all the herringbone gears that available for the gap borrow is necessary to conduct the gap borrowing operation, gear 5 and gear 6 have a significant improvement of wheel diameter by gear gap borrow, but the diameters without gap borrow are large enough for high quantity grinding. At present, the grinding wheel is made of abrasive grain and adhesive by pressing or sintering, too large diameter after the gap borrow will weaken the wheel strength[8]. On the contrary, the above situation shows that the undercut design widths of herringbone gear 5 and gear 6 are too large, and there is a reduction room for optimization. Taking in to account the allowable limit of typical grinding machine and wheel specification, the largest allowable diameter D_A of the wheel after dressing is 78mm. when the wheel diameters of gear 5 and gear 6 are limited at 78mm, after numerical simulation, the reductions of undercut design widths L are shown in Table. 5.

Table. 5 Reduction of L under actual grinding wheel diameter D_A

Herringbone	Φ_u(mm)	L(mm)	D_{Max}(mm)	D_A(mm)	L'(mm)	Reduction of L(%)
Gear 5	110.265	20	118.422	78	15.504	22.48
Gear6	370.62	20	100.243	78	16.29	18.55

As shown in Table. 5, on the premise of ensuring sufficient grinding wheel diameter, the undercut width of gear 5 and gear 6 can be reduced by 22.48% and 18.55% respectively. For the large size herringbone gear, the reduction in undercut width will have significant benefits for weight reduction

design and space utilization of individual parts or components, even entire systems.

Besides, as shown in Table. 4, not all the herringbone gears that available for the gap borrow are suitable for the operation, the gap borrowing efficiency of gear 7 and gear 8 are not significant, even results in negative effects due to the interference of wheel thickness. In gear 7 and gear 8, the gap borrowing parameter K=0.749 is too close to the boundary K_a=0.747, so the safety margin δ in set (4) should be at least 0.002 to limit the gap borrow condition of gear 7 and gear 8. New K_a=0.749 will refuse gear 7 and gear 8 to borrow gear gap.

As shown in Fig. 14, when the tooth side gaps J_t =0 and safety margin δ=0, by gear gap borrowing, most herringbone gears available for gear gap borrow grinding have a significant effect on grinding wheel diameter expansion in theory. Every herringbone gear available for gear gap borrow has its own optimal space borrowing interval of K, the efficiency of grinding wheel diameter expansion in the optimal interval is significantly higher.

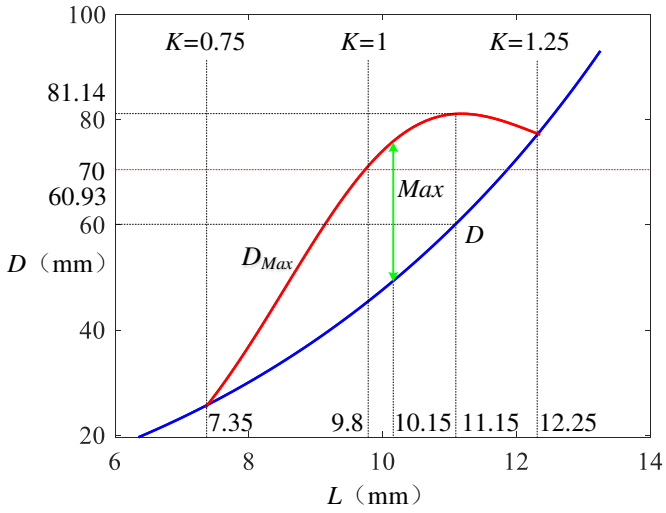

Fig. 14 Gear gap space borrow efficiency in theory

4. Conclusions

The main contributions and key conclusions of this paper are as follow.

1. The gap space borrow grinding method for herringbone gear was proposed and verified.

2. The judgement and method of borrow gap grinding condition for herringbone gear was and the design method of borrow gap grinding herringbone gear based on undercut width was completed and verified.

3. The analysis models of the herringbone gear undercut width and the grinding wheel maximum diameter were built and verified.

4. Part of herringbone gears can extend grinding wheel diameter by reducing undercut width based on borrow gap grinding method.

5. Every herringbone gear available for gear gap borrow has its own high efficiency expansion interval of wheel diameter.

Reference

[1]. Ning Zhao; Linlin Sun; Bibo Fu; Haifeng Li. Web Structural Optimization of the Big Aviation Herringbone Gear Based on APDL Language. [J] Applied Mechanics and Materials. 2014. 487(1):

692-698.

[2]. Sagar Patil; Prashant Ambhore. Design and Analysis Herringbone Gear Use in Industry. [C] ICRRM2019-System Reliability, Quantity Control, Safety, Maintenance and Management. 2020: 53-59.

[3]. Ke Li. Herringbone Gear Meshing Force Simulation Based on UG and ADAMS. [J] Applied Mechanics and Materials. 2014 532(532): 320-323.

[4]. Feng, G.; Gu, Y.; Lan, X.; Zhou, M. Geometric Design and Characteristic Analysis of Herringbone Face Gears. [J] Journal of Tsinghua University. 2019.59(8): 670-682.

[5]. Shangjun Ma; Geng Liu; Liyan Wu; Lidong Jiang. Virtual Assembly and Accurate Parameterized Modeling of Herringbone Gearing. [J] Computer Simulation.2009. 26(3): 294-297.

[6]. Yan Yuesheng; Zhang Xijing; Jia Chao. Optimization Design of Modification of Herringbone Star Gear Transmission. [J] Mechanic Transmission. 2017. 42(11): 85-88.

[7]. Wei Liu; Lunqin Duan; Runjiao Wang; Yanyan Wang. Analysis of Mesh Stiffness of Herringbone Gear Considering Modification. [C] Journal of Physics: Conference Series. 2019: 1-12.

[8]. Zina Pavloushova; David Jech, Pavel Komarov; Ivana Rocnakova; Lucie Dyckova; Michaela Remesova; Ladislav Celko; Daniel Holemy. Characterization of High-Speed Aluminum Abrasive Grinding Wheel. [J] Materials Science & Engineering. 2020. 405(11): 365-369.

Declarations

- Availability of data and materials

All data and materials have been included in the article, and any other information can be provided according to your subsequent requirements.

- Competing interests

We declare that we have no financial and personal relationships with other people or organizations that can inappropriately influence our work, there is no professional or other personal interest of any nature or kind in any product, service and/or company that could be construed as influencing the position presented in, or the review of, the manuscript entitled.

- Funding

This study is completed in combination with production and supported by confidential secret projects within AECC. At present, there are no other publicly available projects to support this study.

- Authors' contributions

Zemin Zhao (First Author, Corresponding Author): undertook the main writing and tasks of the article, pre research, visualization, mathematical modeling and derivation, experimental planning and operation.
Xingfu Zhao: provided the initial theory, Conceptualization research direction, main research ideas and financial support.
Hao Sun: provided important advice and help for the research ideas of this paper and the implementation of the experiment.
Chao Dong: undertook the coordination of experimental resources and put forward important suggestions for the simulation part.
Chunlei Wang: provided important revision suggestions, implementation and operation suggestions of the experimental part and coordination of the experimental equipment.
Shancheng Wang and Hongyan Zhang: provided key writing and research suggestions, as well as the supervision of the writing progress of the paper.

- Acknowledgements

Thanks to the financial and technical support provided by the authors who jointly completed this article.

Availability of data and materials

The data supporting the results reported is in Table 2 and Table 3, which comes from machining experiments and simulation based on verification.